Electronic Supplementary Material (ESI) for Journal of Materials Chemistry B.

An electrochemical bifunctional sensor for the detection of nitrite and hydrogen peroxide based on layer-by-layer multilayer films of cationic phthalocyanine cobalt (II) and carbon Nanotubes

Jialin Zhang,[a] Zhimin Chen,[a] Hao Wu,[a] Feng Wu,[a] Chunying He,[a] Bin Wang,[a] Yiqun Wu,[a, b] and Zhiyu Ren*[a]*

[a] Key Laboratory of Functional Inorganic Material Chemistry (Ministry of Education of China), School of Chemistry and Materials Science, Heilongjiang University, 74# Xuefu Road, Nangang District, Harbin 150080, People's Republic of China;

[b] Shanghai Institutes of Optics and Fine Mechanics, Chinese Academy of Sciences, 390# Qinghe Road, Jiading District, Shanghai 201800, People's Republic of China.

Corresponding author E-mail: zmchen@siom.ac.cn, zyren@hlju.edu.cn

Tel.: +86 451 86604331,

Fax: +86 451 86608616

1. Synthesis of 2,9,16,23-tetra[4-(N- methyl)pyridinyloxy] phthalocyanine cobalt(Ⅱ) sulfate ([TMPyPcCo](SO$_4$)$_2$)

The synthetic scheme of [TMPyPcCo](SO$_4$)$_2$ is shown in scheme S1.[1]

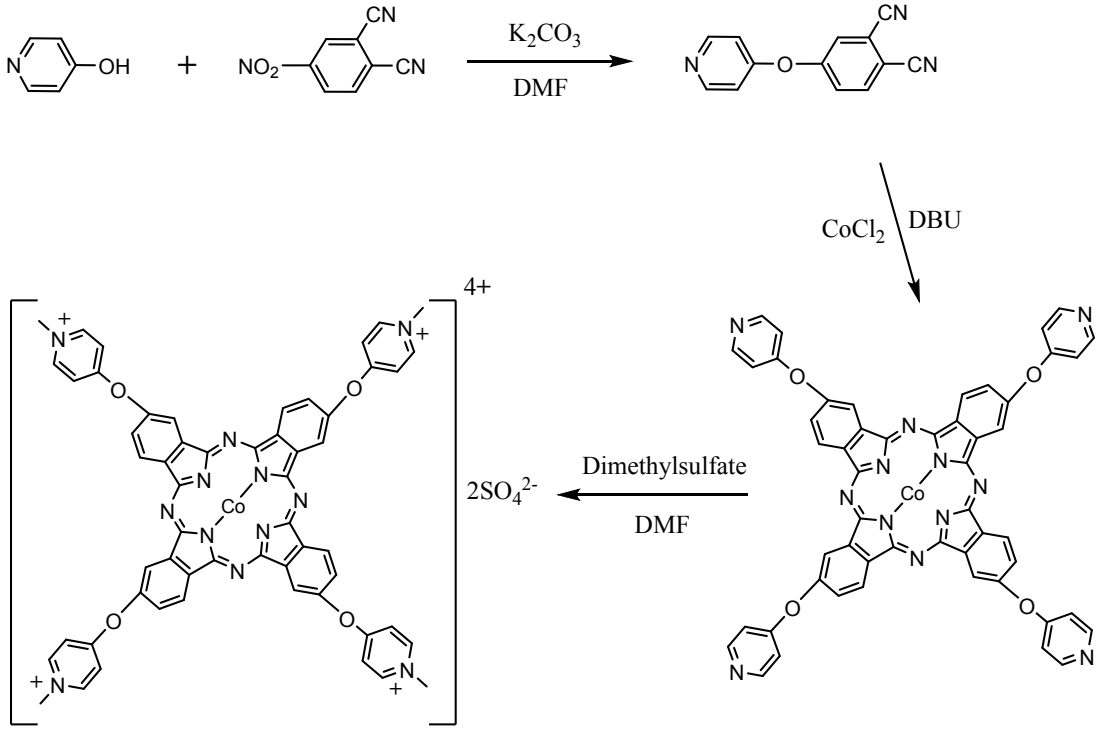

Scheme S1. Synthetical scheme of 2,9,16,23-tetra[4-(N- methyl) pyridinyloxy] phthalocyanine cobalt(Ⅱ) sulfate

1.1 Synthesis of 4-(Pyridine-4-yloxy) phthalonitrile

4-Nitrophthalonitrile (0.07 mol, 12.24 g) and 4-hydroxypyridine (0.08 mol, 8.04 g) were stirred with dry dimethylformamide (100 mL) under nitrogen at room temperature, while anhydrous potassium carbonate (0.086 mol, 12.0 g) was added every 10 hours in three equal lots. The mixture was stirred efficiently for further 5 days, and then poured into ice-water (100 mL) with stirring. The resulting precipitate was collected by filtration, washed with distilled water and then vacuum dried. The rough product was further purified by silica gel column chromatography, eluting with trichloromethane /acetone (5 : 1, V/V), eventually to form white crystals. Yield: 9.33 g (72.43%). ^{1}H NMR ($CDCl_3$, TMS, δ ppm): 2.76 (s, 6H, CH_3), 8.03(d, 1H, Ar), 7.85 (d, 1H, Ar), 7.62 (d, 2H, Py) , 7.54 (s, 1H, Ar), 6.58 (d, 2H, Py).

1. 2 Synthesis of 2,9,16,23- tetra[4- (N- methyl) Pyridinyloxy] phthalocyanine cobalt(Ⅱ) sulfate ([TMPyPcCo]$^{4+}$)

4-(Pyridine-4-yloxy)phthalonitrile (0.008 mol, 1.70 g), anhydrous cobalt (II) chloride (0.004 mol, 0.49 g) and 1,8-dicyanobicycio-[5.4.0]-undec-7-ene (DBU) (0.014 mol, 2 mL) were heated in freshly distilled 1-pentanol (50 mL) at reflux temperature for 12 h under nitrogen. After cooling to room temperature, the precipitate was filtered, washed successively with methanol (50 mL) and acetone (50 mL), and then dissolved in dry dimethylformamide (10 mL) while heating to 120 ºC. After adding a few drops of dimethyl sulfate (0.5 mL, 0.0053 mol), the reaction mixture was stirred continuously at 120 ºC for 12 h. After that, the solution was poured into hot acetone (15 mL) and the resultant solid collected by filtration and washed thoroughly with acetone. The filter-cake was dried in a vacuum oven at 50 ºC for 1 h, affording dark purple powders. Yield: 0.90 g (39.42%). MALDI-MS Calcd (Found): m/z= 1003.26 (1003.21) [M^+].

1.3 The pretreatment of the substrates

The glassy carbon electrode (GCE, diameter 4 mm) and indium tin oxide (ITO) coated glass (3.0 cm×1.0 cm) were used as substrates for electrochemical measurement and characterization. The GCE substrates were polished with 1.0, 0.3 and 0.05 μm aluminum oxide powder successively and ultrasonically washed with ethanol and distilled water for 1 min, respectively. The ITO glass substrates were cleaned by sonication in a series of solvents, acetone, ethanol, and deionized water, for 30 min each. Then the substrates were electrochemical activation, which performed as follows: first, the substrates were immersed in the PBS solution and cleaned by cyclic voltammetry between - 0.5 and + 1.2 V at 50 mV s^{-1} until a stable profile was obtained, then the substrates were oxidized at 2.0 V for 60 s followed by reduction at−1.1 V for 30 s. Finally, the pretreated substrates were dried with nitrogen gas and used for modification immediately.

1.4 The detection limit (LOD) calculation method

For a linear calibration curve, it can be expressed in a model such as y = b + kx. This model is used to compute the sensitivity b and the LOD. Therefore, the LOD can be expressed as LOD = 3 S/k, where S is the standard deviation of the background

current response and k is the sensitivity, which is the slope of the calibration curve. When calculating the S, the background current response is necessary. More than 11 values of the matrix blank responses are selected. This method can be applied in all cases, and it is most applicable when the analysis method does not involve background noise.[2, 3]

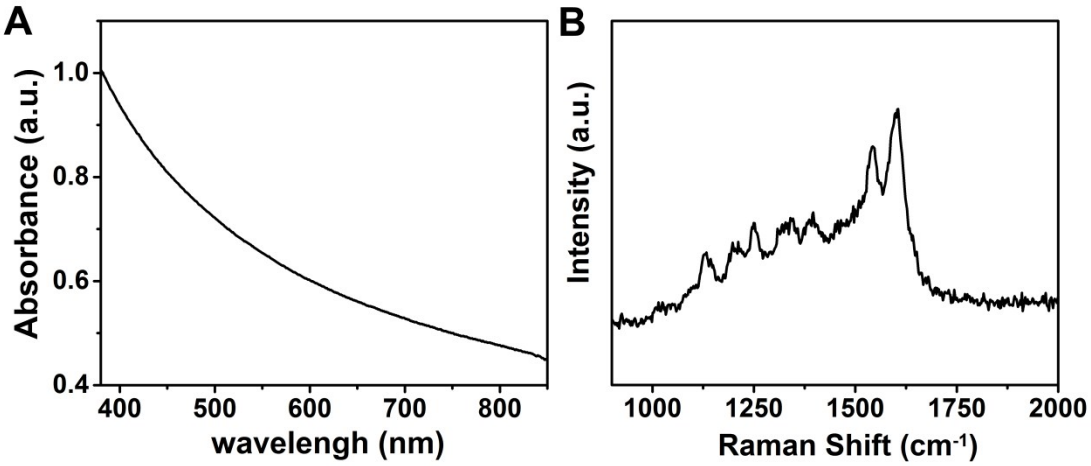

Fig. S1 (A) UV-vis absorption spectrum of aCNTs dispersed in aqueous solution; (B) the Raman spectrum of pure [TMPyPcCo]$(SO_4)_2$ film.

In the Raman spectrum of [TMPyPcCo]$(SO_4)_2$ (Fig. S1 **(**B**)**), two mainly peaks at 1393 cm^{-1} and 1544 cm^{-1} correspond to the symmetry B_{1g} modes; while the weak peaks at 1129 cm^{-1} and 1245 cm^{-1} is attributed to B_{2g} active modes. The nondegenerate B_{1g} and B_{2g} modes are in-plane vibrations.[4,5]

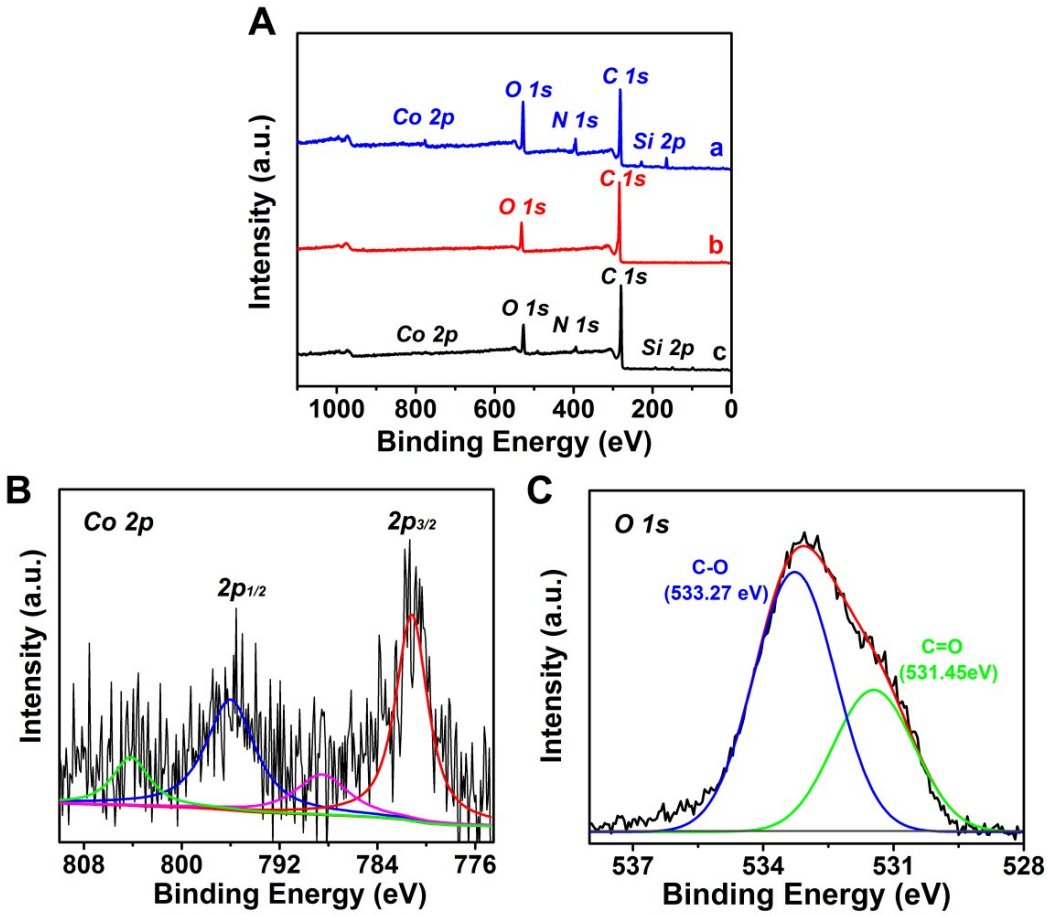

Fig. S2 (A) The survey spectra of $[TMPyPcCo](SO_4)_2$ (a), aCNTs (b), and $[TMPyPcCo/aCNTs]_{12}$ film on ITO substrate (c); (B and C) the high-resolution *Co2p* and *O1s* XPS of $[TMPyPcCo/aCNTs]_{12}$ film, respectively.

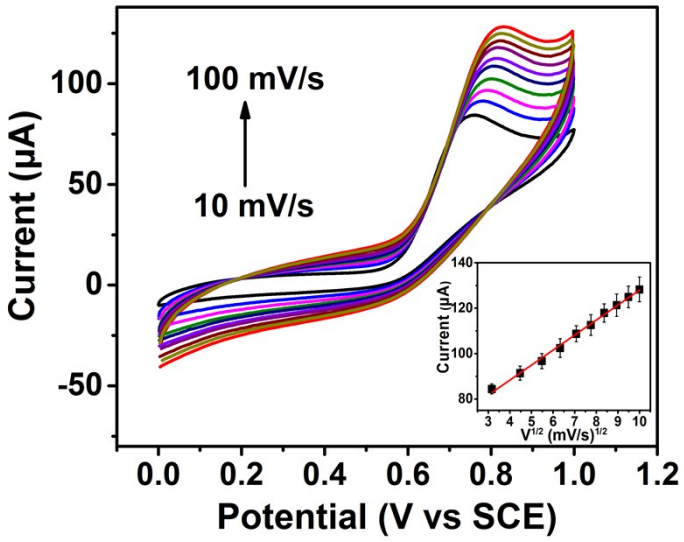

Fig. S3 CVs of the $[TMPyPcCo/aCNTs]_{12}$/GCE in 0.1 M PBS (pH = 6.2) solution containing 1 mM NO_2^- measured at different scan rates (10-100 $mV \cdot s^{-1}$). Inset: the calibration plots between the anodic peak currents *vs.* the scan rate ($I_{pa} = 1.32061 \times v^{1/2} + 12.388$ (μA, $mV^{1/2} \cdot s^{-1/2}$), $R^2 = 0.996$; I_{pa} and V are anodic peak current and scan rate, respectively).

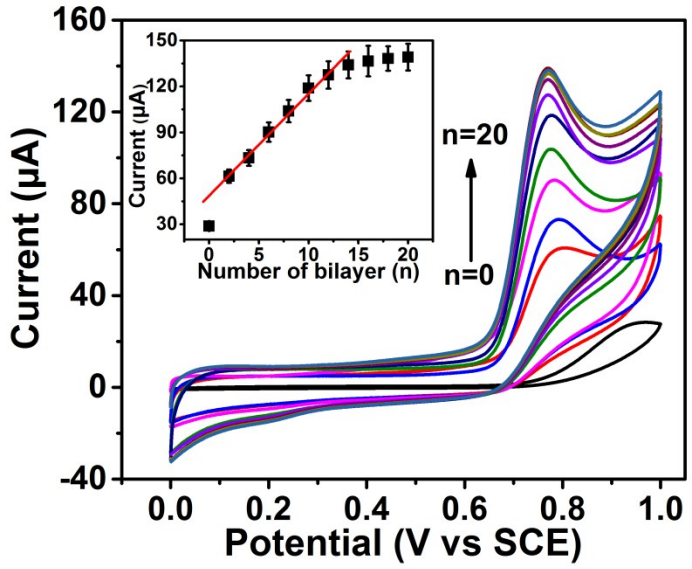

Fig. S4 CVs of the $[TMPyPcCo/aCNTs]_n$/GCE (n = 2-20) in 0.1 M PBS (pH = 6.2) solution containing 1 mM NO_2^-, scan rate: 50 $mV \cdot s^{-1}$. Inset: The corresponding linear calibration relationship of the current response of 1 mM NO_2^- *vs.* n.

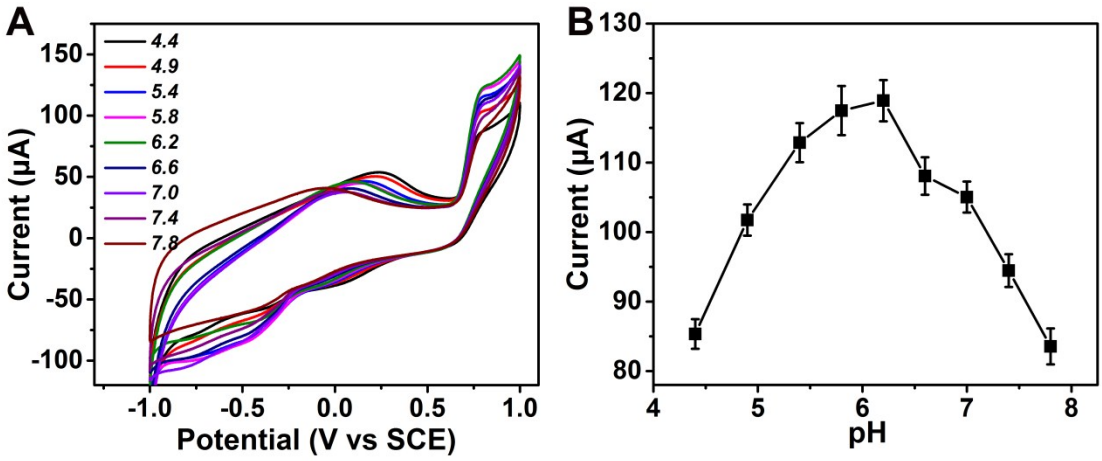

Fig. S5 (A) CVs of $[TMPyPcCo/aCNTs]_{12}$/GCE in 0.1 M PBS solution containing 1 mM NO_2^- at different pH value, scan rate: 50 $mV \cdot s^{-1}$; (B) the relation between the oxidation peak currents and the pH values.

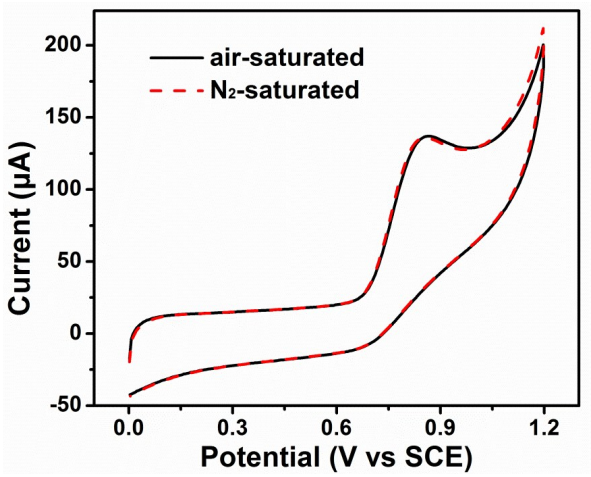

Fig. S6 CVs of $[TMPyPcCo/aCNTs]_{12}$/GCE in 0.1 M PBS solution containing 1 mM NO_2^- (pH = 6.2) (scan rate: 50 $mV \cdot s^{-1}$), N_2-saturated solution (red dashed line) and air-saturated solution (black line).

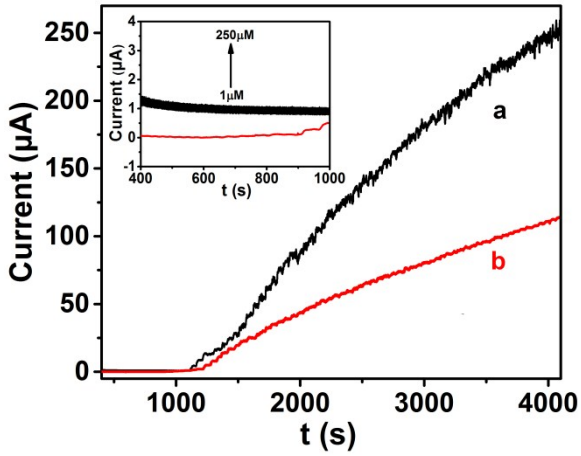

Fig. S7 Amperometric response of the [TMPyPcCo]$(SO_4)_2$/GCE (red line) and aCNTs/GCE (black line) (holding at 0.7 V vs. SCE) for the successive additions of 0.5 mM to 30 mM NO_2^- into continuously stirred 0.1 M PBS (pH = 6.2).

Table S1 Comparison of the sensing performance of different NO_2^- electrochemical sensors

Electrode	Sensitivity (μA/mM)	Linear range (μM)	Limit detection (μM)	Ref.
Fe_2O_3/rGO	204	0.05-780	0.015	[6]
GC/TiNnp/NH_2-IL/Hb[a]	27	0.1-2000	0.1	[7]
GCE/MTpAP/cit-AuNPs	—	0.5-4700	0.06	[8]
Ag-Au microtrench electrodes	—	200-1400	24	[9]
Cu/f-RGO/GCE[b]	81.6	0.15-10500	0.06	[10]
PEDOT-HMF[c]	382.8	50-7500	0.59	[11]
f-ZnO@rFGO	0.3809	10-8000	33	[12]
Hb/Au/GACS/GCE[d]	9.3	0.05-1000	0.1	[13]
RGO-MWCNT-Pt/Mb[e]	11.7	1-12000	0.93	[14]
SiO_2/C/MnPc	17300	0.79-15.74	0.02	[15]
Au-RGO/PDDA	473.5	0.096-340	0.062	[16]
CoPcF-MWCNTs	29.9	0.096-340	0.062	[17]
TOAB/ZnPp-C60/GCE[f]	215.6	2-164	1.44	[18]

Fe_2O_3-CoO	—	0.2-16200	0.1	[19]
PDDA-rGO	—	0.5-2000	0.2	[20]
Au-Pd/rGO	—	0.05-1000	0.02	[21]
[TMPyPcCo/aCNTs]$_{12}$	***18***	***5-30000***	***2.6***	***This work***

Remark: a) glassy carbon/titanium nitrite nanoparticles/amine-terminated ionic liquid/hemoglobin; b) Cu particles/flower-like reduced graphene oxide/glassy carbon electrode; c) poly(3,4-ethylenedioxythiophene) hollowmicroflowers; d) flower-like zinc oxide/reduced functionalized graphene oxide; e) reduced graphene oxide- multiwalled carbonnanotubes-platinum nanoparticles/myoglobin; f) tetraoctylammonium bromide/zinc porphyrin−fullerene/glassy carbon electrode.

Table S2 Comparison of the analytical performance of other methods for detecting NO_2^-.

System	Sensitivity	Linear range (μM)	Limit detection (μM)	Ref.
chemiluminescence	—	0.056-0.21	—	[22]
Spectrophotometry	—	0.0145-1.45	6.6×10^{-3}	[23]
capillary electrophoresis	—	0.145-72.46	0.13	[24]
Microchip Electrophoresis	42.1 pA/μM	10-250	1	[25]
HPLC with UV/vis	—	0.359	14.4	[26]
HPLC with UV/vis	—	1-100	—	[27]
IL-DLLME-HPLC	—	5.79×10^{-3}-7.24	7.24×10^{-4}	[28]

Table S3. Determination of NO_2^- in water samples.

Sample	Added (mM)	Found (mM)	Recovery (%)	RSD (%) (n=3)
1	0.5	0.5155	103.1	3.57
2	3	3.033	101.1	3.15
3	10	10.62	106.2	2.59
4	20	20.18	100.9	3.78

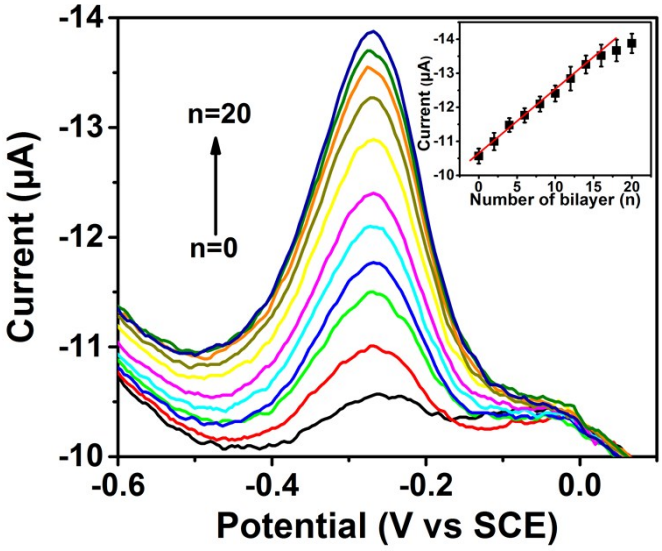

Fig. S8 DPVs of the $[TMPyPcCo/aCNTs]_n$/GCE (n = 0-20) in 0.1 M PBS (pH = 7.0) solution containing 1 mM H_2O_2. Inset: The corresponding linear calibration relationship of the current response of 1 mM H_2O_2 *vs.* n.

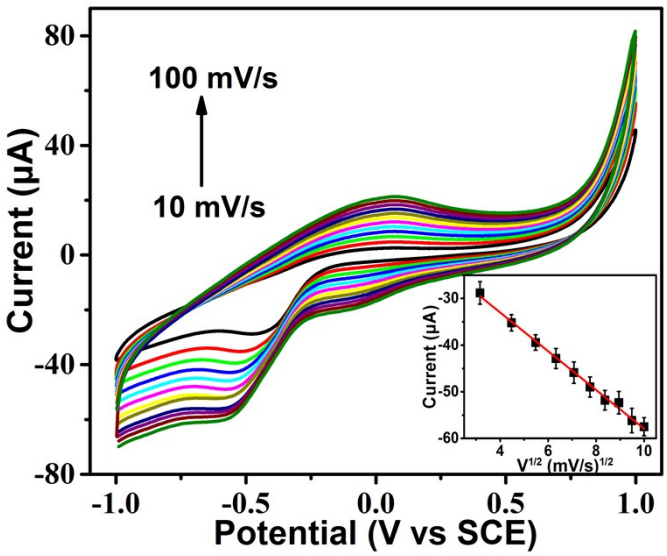

Fig. S9 CVs of the $[TMPyPcCo/aCNTs]_{12}$/GCE in 0.1 M PBS (pH = 7.0) solution containing 1 mM H_2O_2 measured at different scan rates (10-100 $mV \cdot s^{-1}$). Inset: the calibration plots between the anodic peak currents *vs.* the scan rate ($Ipc = -4.1546 \times V^{1/2} - 16.38188$ (μA, $mV^{1/2} \cdot s^{-1/2}$, $R^2 = 0.996$); Ipc and V are cathode peak current and scan rate, respectively).

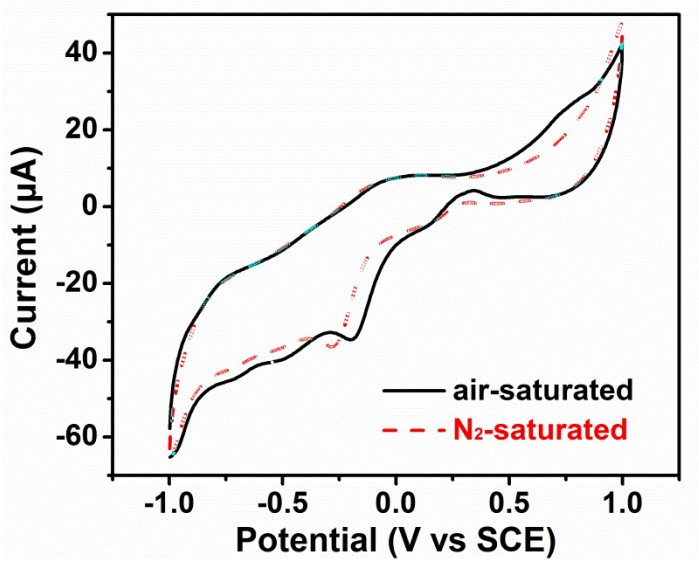

Fig. S10 CVs of $[TMPyPcCo/aCNTs]_{12}$/GCE in 0.1 M PBS solution containing 1 mM H_2O_2 (pH = 7.0) (scan rate: 50 $mV \cdot s^{-1}$), N_2-saturated solution (red line) and air-saturated solution (black dashed line).

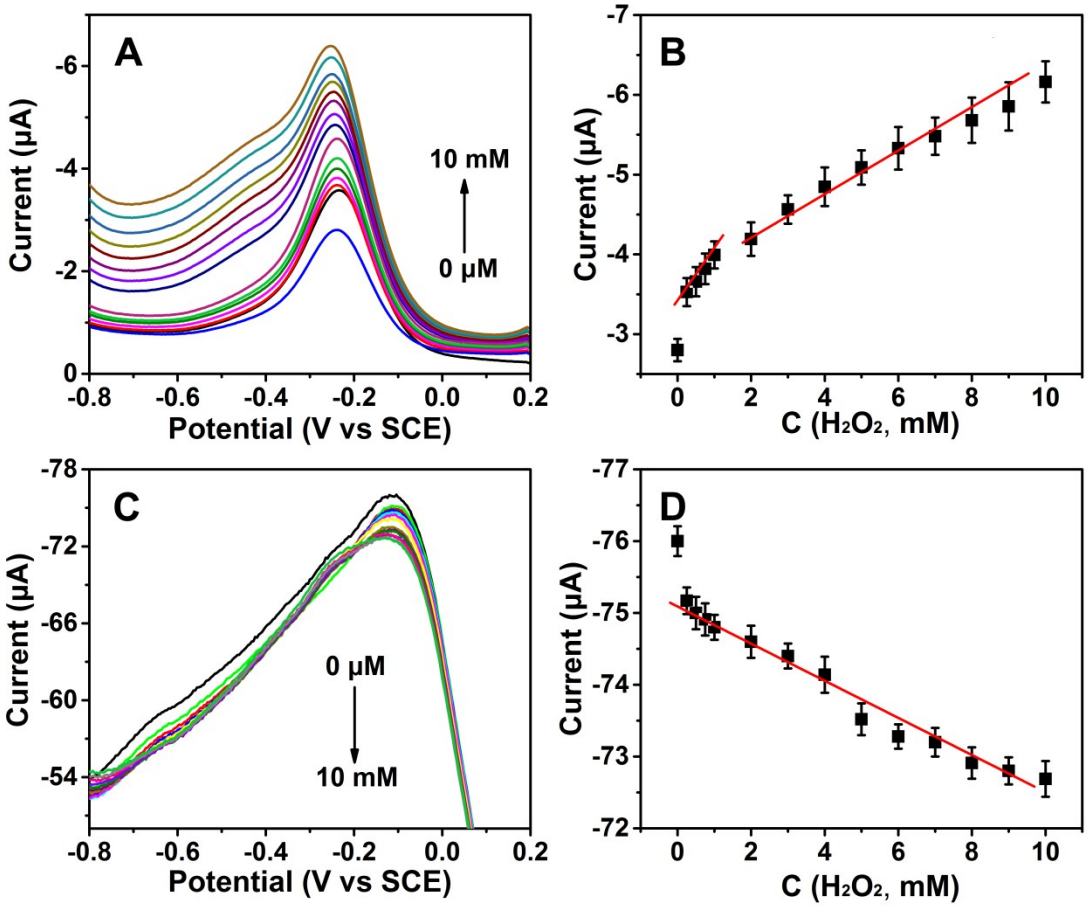

Fig. S11 (A) DPVs response for different concentration of H_2O_2 at the [TMPyPcCo]$(SO_4)_2$/GCE in 0.1M PBS solution (pH = 7.0); (B) the calibration linear relationship of the current response *vs.* the H_2O_2 concentration for [TMPyPcCo]$(SO_4)_2$/GCE: I (H_2O_2, μA) = -0.628 (μA·mM^{-1}) × C (mM) - 3.3603 (0-1 mM, R^2 = 0.993), and I (H_2O_2, μA) = -0.230 (μA·mM^{-1}) × C (mM) - 3.862803 (1-9 mM, R^2 = 0.985); (C) DPVs response for different concentration of H_2O_2 at the aCNTs/GCE in 0.1M PBS solution (pH = 7.0); (D) the calibration linear relationship of the current response *vs.* the H_2O_2 concentration for aCNTs/GCE: I (H_2O_2, μA) = 0.291 (μA·mM^{-1}) × C (mM) - 75.26 (0-9mM, R^2 = 0.932).

Table S4 Comparison of the analytical performance of different H_2O_2 electrochemical sensors

System	Sensitivity (μA/mM)	Linear range (μM)	Limit detection (μM)	Ref.
CNF/H/GC[g]	0.157	50-1000	2	[29]
GCE/[MWCNT-Fe:H_2N-CHIT][h]	50	5-500 50-2500	2.3 9.7	[30]
CuS/CS/GCE[i]	36.4	1-100	0.3	[32]
OMCN-800/GCE[j]	45.41	0.5-1000	0.18	[32]
Hb-PpPDA@Fe_3O_4	76	0.5-400	0.21	[33]
SPAuE-PA-SWCNT-MnTAPc[c]	5.6×10^{-5}	1-30	0.1	[34]
AuNPs/PANI/HNTs[k]	—	10-1000	0.972	[35]
II/CPE[l]	11293	1.14-1120	0.27	[36]
PtNPs/poly-melamine/GCE	32.3	5-1650	0.65	[37]
Ag NF/GCE	19.73	10-16500	4	[38]
Ag/ZIF8/CPE[m]	50.05	20-10000	6.2	[39]
Cyt.c/Ni foam[n]	1.95	0.5-120000	0.2	[40]
CQDs/octahedral Cu_2O	9.021	5-5300	2.8	[41]
Polystyrene@RGO–Pt	67.5	0.5-8000	0.1	[42]
RGO–PtNPs/GCE	22.6	0.05-750.6	0.016	[43]
[TMPyPcCo/aCNTs]$_{12}$	***1.61***	***10-9000***	***2.8***	***This work***

Remark: g) carbon nanofiber-COOH/Glassy carbon; h) Glassy carbon/ multiwalled carbon nanotube–chitosan biopolymer; i) CuS NPs/chitosanmodified glassy carbon electrode; g) ordered mesoporous carbon nitride-800 ºC/glassy carbon electrode; k) gold nanoparticles/polyaniline/ halloysite nanotubes; l) SiO_2–pro–NH–cyanuric–NH_2/carbon paste electrode; m) Ag/Zeolitic imidazolate framework-8/ carbon paste electrode; n) cytochrome c/3D porous nickel foam.

Table S5 Comparison of the analytical performance of other methods for detecting H_2O_2.

Method	Sensitivity	Linear range (μM)	Limit detection (μM)	Ref.
Fluorimetry	—	0-8	0.13	[44]
Spectrophotometry	—	0.2-10	0.2	[45]
Spectrophotometry	—	1-20	0.4	[46]
Fluorimetry	—	5-200	0.34	[47]
chemiluminescence	—	0.5-400	0.1	[48]
chemiluminescence	—	10-50	—	[49]

Table S6. Determination of H_2O_2 in water samples.

Sample	Added (mM)	Found (mM)	Recovery (%)	RSD (%) (n=3)
1	0.1	0.0953	95.3	4.12
2	1	1.003	100.3	3.11
3	4	4.361	109.0	3.24
4	7	7.301	104.3	2.96

References

[1] T. T. Tasso, T. Furuyama, N. Kobayashi, *Inorg. Chem.*, 2013, **52**, 9206-9215.

[2] K. Hasebe, J. Osteryoung, *Anal. Chem.*, 1975, **47** (14), 2412-2418.

[3] A, Shrivastava, V. B. Gupta, *Chron. Young Sci.*, 2011, **2**(1), 21-25.

[4] M. Szybowicz, W.Bała, S. Dümecke, K. Fabisiak, K. Paprocki, M. Drozdowski, *Thin Solid Films*, 2011, **520**, 623–627.

[5] M. Szybowicz, T. Runka, M. Drozdowski, W. Bała, A. Grodzicki, P. Piszczek, A. Bratkowski, *J. Mol. Struct.*, 2004, **704**, 107–113.

[6] S. Radhakrishnan, K .Krishnamoorthy, C. Sekar , J. Wilson, S. J .Kim, *Appl. Catal. B: Environ*, 2014, **148-149**, 22-28.

[7] S. Saadati, A. Salimi, R. Hallaj, A. Rostami, *Sensor. Actuat. B-Chem.*, 2014, **191**, 625-633.

[8] P. Muthukumar, S. A. John, *J. Colloid Interf. Sci.*, 2014, **421**, 78-84.

[9] A. J. Gross, S. Holmes, S. E. C. Dale, M. J. Smallwood, S. J. Green, C. P. Winlove, N. Benjamin, P. G. Winyard, F. Marken, *Talanta*, 2015, **131**, 228-235.

[10] H. W. Wang, C. Q. Wang, B. B. Yang, C. Y. Zhai, D. Bin, K. Zhang, P. Yang, Y. K. Du, *Analyst*, 2015, **140**, 1291-1297.

[11] Y. H. Cheng, C. W. Kung, L. Y. Chou, R. Vittal, K. C. Ho, *Sensor. Actuat. B-Chem.*, 2014, **192**, 762-768.

[12] A. R. Marlinda, A. Pandikumar, N. Yusoff, N. M. Huang, H. N. Lim, *Microchim Acta*, 2015, **182**, 1113-1122.

[13] J. J. Jiang, W. J. Fan, X. Z. Du, *Biosens. Bioelectron.*, 2014, **51**, 343-348.

[14] V. Mani, B. Dinesh, S. M. Chen, R. Saraswathi, *Biosens. Bioelectron*., 2014, **53**, 420-427.

[15] A. Rahim, L. S. S. Santos, S. B. A. Barros, L. T. Kubota, R. Landers, Y. Gushikem, *Electroanalysis*, 2014, **26**, 541-547.

[16] S. F. Jiao, J. Jina, L. Wang, *Sensor. Actuat. B-Chem.*, 2015, **208**, 36-42.

[17] P. Li, Y. Ding, A. Wang, L. Zhou, S. H. Wei, Y. M. Zhou, Y. W. Tang, Y. Chen,C. X. Cai, T. H. Lu, *ACS Appl. Mater. Interfaces*, 2013, **5**, 2255-2260.

[18] H. Wu, S. H. Fan, X. Y. Jin, H. Zhang, H. Chen, Z. Dai, X. Y. Zou, *Anal. Chem.*, 2014, **86**, 6285-6290.

[19] J. P. Wang, D. Y. Zhao, Y. Zhang, J. F. Li, C. X. Xu, *Anal. Methods*, 2014, **6**, 3147-3151.

[20] F. G. Xu, M. Deng, Y. Liu, X. C. Ling, X. Y. Deng, L.Wang., *Electrochem. Commun.*, 2014, **47**, 33-36.

[21] S. S. Li, Y. Y. Hu, A. J. Wang, X. X. Weng, J. R. Chen, J. J. Feng, *Sensor. Actuat. B-Chem.*, 2015, **208**, 468-474.

[22] E. Nagababu, J. M. Rifkind, *Free Radical Bio. Med.*, 2007, **42**, 1146-1154.

[23] M. Miró,W. Frenzel, V. Cerdà, J.M. Estela, *Anal. Chim. Acta*, 2001, **437**, 55-65.

[24] E. Martínková, T. Křžek, P. Coufal, *Chem. Pap.*, 2014, **68**(8), 1008-1014.

[25] R. Kikura-Hanajiri, R. S. Martin, S. M. Lunte, *Anal. Chem.*, 2002, **74**, 6370-6377.

[26] A. Buldt, U. Karst, *Anal. Chem.*, 1999, **71**, 3003-3007.

[27] A. Sharma, K. Raghavendra, T. Adak, A. P. Dash, *Malaria J.*, 2008, **7**, 71.

[28] L. J. He, K. G. Zhang, C. J. Wang, X. L. Luo, S. S. Zhang, *J. Chromatogr. A*, 2011, **1218**, 3595-3600.

[29] F. Valentini, L. Cristofanelli, M. Carbone, G. Palleschi, *Electrochim. Acta*, 2012, **63**, 37-46.

[30] P. Gayathri, A. S. Kumar, *Chem. Eur. J*. 2013, **19**, 17103-17112.

[31] Y. J. Yang, J. F. Zi, W. K. Li, *Electrochimica Acta*, 2014, **115**, 126-130.

[32] Y. F. Zhang, X. J. Bo, A. Nsabimana, C. Luhana, G. Wang, H. Wang, M. Li, L. P. Guo, *Biosens. Bioelectron.*, 2014, **53**, 250-256.

[33] M. Baghayeri, E. N. Zare, M. M. Lakouraj, *Biosens. Bioelectron.*, 2014, **55**, 259-265.

[34] P. Mashaz, T. Mugadzab, N. Sosiboa, P. Mdluli, S. Vilakazi, T. Nyokongb, *Talanta*, 2011, **85**, 2202-2211.

[35] P. Wang, M. G. Du, M. Zhang, H. Zhu, S. Y. Bao, M. L. Zou, T. T. Yang, *Chem. Eng. J.*, 2014, **248**, 307-314.

[36] A. A. Ensafi, N. Zandi-Atashbar, M. Ghiaci, M. Taghizadeh, B. Rezaei, *Mat. Sci. Eng. C-Mater.*, 2015, **47**, 290-297.

[37] S. J. He, Z. G. Chen, Y. Y. Yu, L. J. Shi, *RSC Adv.*,2014, **4**,45185-45190.

[38] D. W. Li, L. Luo, Z. Y. Pang, X. D. Chen, Y. B. Cai, Q. F. Wei, *RSC Adv.,* 2014, **4**, 3857-3863.

[39] A. Samadi-Maybodi, S. Ghasemi, H. Ghaffari-Rad, *Electrochim. Acta*, 2015, **163**, 280-287.

[40] N. Akhtar, S. A. El-Safty, M. Khairy,W. A. El-Said, *Sensor. Actuat. B-Chem.*, 2015, **207**, 158-166.

[41] Y. C. Li, Y. M. Zhong, Y. Y. Zhang, W. Weng, S. X. Li, *Sensor. Actuat. B-Chem.*, 2015, **206**, 735-743.

[42] W. L. Liu, C. Li, P. Zhang, L. Tang, Y. Gu,Y. J. Zhang, J. Q. Zhang, Z. B. Liu, G. X. Sun, Z. Q. Zhang, *RSC Adv.*,2015, **5**, 73993-74002.

[43] S. Palanisamy, H. F. Lee, S. M. Chen, B. Thirumalraj, *RSC Adv.*, 2015, **5**, 105567-105573.

[44] Y. F. Huan, Q. Fei, H. Y. Shan, B. J. Wang, H. Xua, G. D. Feng, *Analyst*, 2015, **140**, 1655-1661.

[45] Z. C. Xing, J. Q. Tian, A. M. Asiri, A. H. Qusti, A. O. Al-Youbi, X. P. Sun, *Biosens. Bioelectron.*, 2014, **52**, 452-457.

[46] Y. W. Zhang, J. Q. Tian, S. Liu, L. Wang, X. Y. Qin, W. B. Lu, G. H. Chang, Y. L. Luo, A. M. Asiri, A. O. Al-Youbi, X. P. Sun, *Analyst*, 2012, **137**, 1325-1328.

[47] A. L. Hu, Y. H. Liu, H. H. Deng, G. L. Hong, A. L. Liu, X. H. Lin, X. H. Xia, W. Chen, *Biosens. Bioelectron.*, 2014, **61**,374-378.

[48] Y. D. Lee, C. K. Lim, A. Singh, J. Koh, J. Kim, I. C. Kwon, S. Kim, *ACS Nano*, 2012, **6** (8), 6759-6766.

[49] M. J. Chaichi, S. N. Azizi, M. Heidarpour, O. Aalijanpour, M. Qandalee, *J Fluoresc.*, 2012, **22**, 1209-1216.